



**HAL**  
open science

## Assessment of fish freshness based on fluorescence measurement of mitochondrial membrane potential

Jérôme Cléach, Méline Soret, Thierry Grard, Philippe Lencel

► **To cite this version:**

Jérôme Cléach, Méline Soret, Thierry Grard, Philippe Lencel. Assessment of fish freshness based on fluorescence measurement of mitochondrial membrane potential. *Food Control*, 2020, 115, pp.107301. 10.1016/j.foodcont.2020.107301 . hal-03490842

**HAL Id: hal-03490842**

**<https://hal.science/hal-03490842v1>**

Submitted on 22 Aug 2022

**HAL** is a multi-disciplinary open access archive for the deposit and dissemination of scientific research documents, whether they are published or not. The documents may come from teaching and research institutions in France or abroad, or from public or private research centers.

L'archive ouverte pluridisciplinaire **HAL**, est destinée au dépôt et à la diffusion de documents scientifiques de niveau recherche, publiés ou non, émanant des établissements d'enseignement et de recherche français ou étrangers, des laboratoires publics ou privés.



Distributed under a Creative Commons Attribution - NonCommercial 4.0 International License

1 **Assessment of fish freshness based on fluorescence measurement of**  
2 **mitochondrial membrane potential**

3 Jérôme Cléach<sup>a</sup>, Méline Soret<sup>a</sup>, Thierry Grard<sup>a\*</sup> and Philippe Lencel<sup>a</sup>

4 <sup>a</sup>Univ. Littoral Côte d'Opale, UMR transfrontalière INRAe n°1158 BioEcoAgro, USC  
5 ANSES – ULCO, F-62200 Boulogne-sur-Mer, France

6 Email addresses:

7 Jérôme Cléach: [jerome.cleach@univ-littoral.fr](mailto:jerome.cleach@univ-littoral.fr)

8 Méline Soret: [meline.soret@univ-littoral.fr](mailto:meline.soret@univ-littoral.fr)

9 Philippe Lencel: [philippe.lencel@univ-littoral.fr](mailto:philippe.lencel@univ-littoral.fr)

10 \*Corresponding author: Thierry Grard

11 Tel: +33 3 21 99 25 08; Email address: [thierry.grard@univ-littoral.fr](mailto:thierry.grard@univ-littoral.fr)

12 **Highlights**

13 - Mitochondrial functions of European seabass fillets were disrupted from 96h storage (D4) at  
14 +4°C

15 - Spectral properties of Rh123 and TMRM were correlated to mitochondrial health

16 - The evaluation of mitochondrial bioenergetics represents an early indicator of fish freshness

17 - A micro-volume fluorimeter could be considered for rapid evaluation of fish freshness

18

19 **Key words**

20 Mitochondrial potential; fish freshness; micro-volume fluorimetry

21 **Abstract**

22 Research and development of methods to assess fish freshness continues to be a major  
23 challenge for the fishing industry. At the same time, consumers are now increasingly attentive  
24 to food quality, including fish freshness and product history. Here, we propose a reliable,

25 rapid and easy-to-apply fluorimetric approach to assess fish freshness using a micro-volume  
26 fluorimeter. Mitochondrial functions were assessed in European seabass (*Dicentrarchus*  
27 *labrax*) fillets at different durations of storage at +4°C: from Day 0 to Day 8. We found that  
28 mitochondrial respiration and mitochondrial membrane potential ( $\Delta\Psi_m$ ) were significantly  
29 disrupted after 4 days of storage at +4°C. The spectral properties (emission peak and  
30 fluorescence intensity) of mitochondrial membrane potential probes rhodamine 123 (Rh123)  
31 and tetramethylrhodamine methyl ester (TMRM) were strongly affected by the  $\Delta\Psi_m$  integrity  
32 of the fish fillets. We highlighted two categories of fish quality as a function of  $\Delta\Psi_m$ : Day 0 to  
33 Day 3,  $\Delta\Psi_m$  was preserved; and D4 to D7,  $\Delta\Psi_m$  was disrupted. Thus, evaluation of  $\Delta\Psi_m$   
34 constitutes an early and reliable predictive indicator of fish freshness.

## 35 **1. Introduction**

36 Freshness is an important factor that contributes to fish quality (Olafsdottir, et al., 1997), and  
37 its evaluation is still a major challenge in the fishing industry. Numerous methods and  
38 technologies have been developed to evaluate fish freshness ((Mendes, 2018); (Wu, Pu, &  
39 Sun, 2019) (Cheng, Sun, Han, & Zeng, 2014), (Hassoun & Karoui, 2015)). Current traditional  
40 methods for assessing fish quality are based on physical, chemical, microbiological and  
41 sensory parameters (Rehbein & Oehlenschlager, 2009). However, these methods present  
42 numerous limits. They do not apply to all species, are time consuming, and require special  
43 skills. Consequently, there is still a need in the food industry to develop rapid, reliable and  
44 simple methods to assess fish freshness.

45 Understanding *post mortem* mechanisms in fish muscle cells is essential to identify new  
46 markers, and to develop methods for the evaluation of fish freshness. In a previous study, we  
47 assessed *post mortem* changes in mitochondrial functions and integrity in gilthead seabream  
48 (*Sparus aurata*) fish muscle cells. We demonstrated that mitochondrial respiration and  
49 mitochondrial membrane potential ( $\Delta\Psi_m$ ) were significantly altered after 4 days of storage at

50 +4°C (Jérôme Cléach, et al., 2019). Our data showed, for the first time, that mitochondrial  
51 activity constituted a putative reliable indicator to assess fish freshness at different early *post*  
52 *mortem* time points.

53 In *post mortem* conditions, fish muscle is deprived of oxygen and nutrients, and is  
54 consequently in an ischemic state. In this context, mitochondrial activity is disrupted. Many  
55 methods are available to investigate mitochondrial functions and integrity, such as the  
56 analysis of the mitochondrial respiratory chain by oxygraphy and the evaluation of  
57 mitochondrial membrane potential ( $\Delta\Psi_m$ ) by fluorimetry (Kuznetsov, et al., 2008).  
58 Mitochondrial membrane potential ( $\Delta\Psi_m$ ) and the proton gradient ( $\Delta pH$ ) constitute the  
59 components of the proton motive force (Mitchell, 2011).  $\Delta\Psi_m$  is essential for ADP  
60 phosphorylation and ATP synthase activity.  $\Delta\Psi_m$  is also involved in many less well studied  
61 functions such as: homeostasis, mitochondrial function regulation, and transport of ions,  
62 proteins, and nucleic acids (Zorova, et al., 2018). Therefore, monitoring oxygen consumption  
63 by oxygraphy and evaluation of  $\Delta\Psi_m$  are useful approaches to assess mitochondrial health.

64 The purpose of this study was to correlate *post mortem* mitochondrial bioenergetics with fish  
65 freshness. This study focused on the assessment of  $\Delta\Psi_m$  as a reliable method to determine fish  
66 quality at early *post mortem* time points. We studied the  $\Delta\Psi_m$  values of mitochondria isolated  
67 from European seabass (*Dicentrarchus labrax*) skeletal muscle at different durations of  
68 storage at +4°C to comply with the storage temperatures widely used in seafood processing  
69 companies: from 6 hours after slaughtering (D0) to Day 7. First, in order to validate  
70 mitochondrial extraction and assess mitochondrial respiration, we calculated the respiratory  
71 control index (RCI) at different *post mortem* time points. Then,  $\Delta\Psi_m$  was assessed using a  
72 Nanodrop 3300 micro-volume fluorimeter (MVF). This device has many advantages; for  
73 example, it is small, portable, easy-to-use and to maintain. These features make it ideal for  
74 effective rapid evaluation of fish freshness in the food industry, without the need for special

75 technical skills. In a previous study, we demonstrated the strong capabilities of the MVF to  
76 assess membrane potential with cationic fluorescent probes (J Cléach, et al., 2018). In this  
77 study, we compared the action of two cationic fluorescent probes, traditionally used in the  
78 study of mitochondrial potential: rhodamine 123 (Rh123) and tetramethylrhodamine methyl  
79 ester (TMRM).

## 80 **2. Materials and methods**

### 81 2.1 Reagents

82 4-morpholinepropanesulfonic acid (MOPS), bovine serum albumin (BSA), carbonyl cyanide  
83 3-chlorophenylhydrazone (CCCP), ethylene-bis(oxyethylenitrilo)tetraacetic acid (EGTA),  
84 malate, proteinase type XXIV, rhodamine 123 (Rh123), succinate, tetramethylrhodamine  
85 methyl ester perchlorate (TMRM), and Tris (hydroxymethyl)aminomethane (Trizma<sup>®</sup> base)  
86 were purchased from Sigma-Aldrich (St. Louis, MO, USA). Potassium chloride (KCl) and  
87 glutamate were acquired from Fisher Labosi (Paris, France). Magnesium chloride (MgCl<sub>2</sub>),  
88 potassium dihydrogen phosphate (KH<sub>2</sub>PO<sub>4</sub>) and sucrose were purchased from Acros Organics  
89 (Morris, NJ, USA). Rh123, TMRM and CCCP were prepared in dimethyl sulfoxide (DMSO)  
90 purchased from Thermo Scientific (San Diego, CA, USA).

### 91 2.2 Fish origin and storage

92 The European seabass (*Dicentrarchus labrax*) (300–450 g) used in this study were sourced  
93 from Aquanord sea farm (Gravelines, France), as previously described (Jérôme Cléach, et al.,  
94 2019). This farmed fish model was chosen in order to obtain accurate data on living  
95 conditions, slaughtering, and storage, which can potentially influence the study of freshness.  
96 Upon arrival at the laboratory, the fish were immediately filleted. The fillets were stored on  
97 ice in a cold room (+4°C) for 8 days and used for experiments every 24 h over 8 days: Day 0,  
98 Day 1, Day 2, Day 3, Day 4, Day 5, Day 6, Day 7 and Day 8. The ice was renewed every day.

99 Plastic wrapping was used to avoid contact between the fillets and the ice or the accumulated  
100 water.

### 101 2.3 Isolation of mitochondria from fish fillets

102 The method for mitochondria isolation was adapted from Pasdois, Parker, Griffiths, and  
103 Halestrap (2011). It was also previously used for extraction of gilthead seabream (*Sparus*  
104 *aurata*) skeletal muscle cell mitochondria (Jérôme Cléach, et al., 2019). All the steps in  
105 mitochondrial isolation were performed in a cold room at +4 °C. Fish muscle was dissected  
106 from the fillet (3 g) and finely diced with scissors. The fine pieces obtained (2–3 mm<sup>3</sup>) were  
107 incubated at +4°C for 7 min under stirring in 20 mL of isolation buffer (180 mM KCl, 80 mM  
108 sucrose, 5 mM MgCl<sub>2</sub>, 10 mM Tris, 2 mM EGTA, pH 7.2 at +4°C), supplemented with 0.1  
109 mg.mL<sup>-1</sup> of bacterial proteinase type XXIV. The resulting tissue suspension was poured into a  
110 30 mL glass Potter homogenizer and homogenized for 3 min using a motorized Teflon pestle  
111 at 300 rpm. The homogenate was centrifuged at 7,500 g for 10 min. The resulting pellet was  
112 first washed and then resuspended in 20 mL isolation buffer containing 2 mg.mL<sup>-1</sup> of fatty  
113 acid-free BSA, and homogenized for 3 min at 150 rpm. The homogenate was then centrifuged  
114 at 700 g for 10 min. The supernatant was centrifuged at 1,500 g for 10 min. The resulting  
115 supernatant was centrifuged again at 7,000 g for 10 min. The mitochondrial pellet obtained  
116 was then suspended with a low volume (40 µL) of isolation buffer in order to obtain a  
117 concentrated mitochondrial suspension. The protein concentration was determined using a  
118 Bio-Rad protein assay kit, derived from the method developed by Bradford (1976), with BSA  
119 as a standard. Mitochondria were kept on ice at a final concentration of 60–100 mg.mL<sup>-1</sup> for  
120 not more than 4 h.

### 121 2.4 Respiratory control index (RCI)

122 Oxygraphy (Rank Brothers Digital Model 10, Cambridge, United Kingdom) was used to  
123 monitor mitochondrial functions after isolation by measuring the respiratory control index

124 (RCI) at different days of storage at +4°C (Day 0, Day 1, Day 2, Day 3, Day 4, Day 5, Day 6  
125 and Day 7), as previously described (Jérôme Cléach, et al., 2019). First, 2.1 mL of respiration  
126 buffer (KCl 125 mM, MOPS 20 mM, Tris 10 mM, EGTA 10 µM, KH<sub>2</sub>PO<sub>4</sub> 2.5 mM, fatty  
127 acid-free BSA 2 mg.mL<sup>-1</sup>, pH 7.2) was added to the oxygraph chamber supplemented with  
128 glutamate (5 mM), malate (2 mM), and succinate (5 mM). Then, mitochondria were added at  
129 a final concentration of 0.2 mg.mL<sup>-1</sup>. Oxygen consumption rates were assessed without and  
130 with ADP (1 mM) (basal and state 3, respectively). Then, carboxyatractyloside (CAT) (5 µM)  
131 was added to block the oxygen consumption linked to ATP synthesis. The experiment was  
132 performed at +25°C. Saturating dithionite (Sigma-Aldrich) was added to the oxygraph  
133 chamber to calibrate the device, and to achieve the zero oxygen calibration.

134 RCI was calculated using the following formula:

$$135 \quad RCI = \frac{ADP \text{ (state 3)}}{CAT}$$

136 Where state 3 is the respiration rate during maximum ATP synthesis, and CAT is the  
137 respiration rate not linked to ATP synthesis.

### 138 2.5 Evaluation of mitochondrial membrane potential

139 A NanoDrop 3300 MVF (ThermoFisher Scientific, distributed by Ozyme, Saint-Cyr-l'École,  
140 France) was used to monitor the fluorescence of Rh123 and TMRM in order to evaluate  
141 changes in mitochondrial  $\Delta\Psi_m$  of isolated mitochondria extracted at different storage  
142 durations at +4°C (Day 0, Day 1, Day 2, Day 3, Day 4, Day 5, Day 6 and Day 7). 1 mL of  
143 respiration buffer (KCl 125 mM, MOPS 20 mM, Tris 10 mM, EGTA 10 µM, KH<sub>2</sub>PO<sub>4</sub> 2.5  
144 mM, fatty acid-free BSA 2 mg.mL<sup>-1</sup>, pH 7.2) at +25°C was added to a 5 mL round-bottom  
145 polypropylene tube, originally designed for flow cytometry analysis. Rh123 (50 nM final) or  
146 TMRM (50 nM) were added to the respiratory buffer without respiratory substrates (as a  
147 negative control) or with respiratory substrates: glutamate (5 mM), malate (2 mM), and  
148 succinate (5 mM). Just prior to acquisition, isolated mitochondria were added at a

149 concentration of 0.2 mg.mL<sup>-1</sup>. The decoupling agent CCCP (2 μM final) was then added to  
150 the preparation to disrupt the ΔΨ<sub>m</sub>, leading to Rh123 and TMRM output from the  
151 mitochondria matrix.

152 Rh123 and TMRM were used in quenching mode. At high concentrations (50 – 100 nM),  
153 cationic probes stack inside the mitochondrial matrix to form aggregates leading to the  
154 quenching of the fluorescent emissions of the aggregated molecules (Perry, Norman, Barbieri,  
155 Brown, & Gelbard, 2011).

### 156 2.6 Micro-volume fluorimeter settings

157 The MVF was originally designed to quantify nucleic acids and proteins. However, it is  
158 possible to create and edit methods with the software to study a wide range of fluorophores. In  
159 this way, we created a method to analyze the fluorescence of probes Rh123 and TMRM. The  
160 excitation sources available include: UV LED (excitation maximum 365 nm), Blue LED  
161 (excitation maximum 470 nm), and White LED (460-650 nm excitation). White LED was  
162 selected to study Rh123 and TMRM fluorescence. The virtual emission filter interval (Δλ)  
163 was set at ± 20 nm. 2 μL of sample were used to measure the fluorescence intensity. The  
164 assay blank was carried out with the respiratory buffer. For each sample, 5 measures were  
165 acquired, as recommended by the manufacturer. Importantly, this experimental approach did  
166 not enable the user to measure ΔΨ<sub>m</sub>, but gave a degree of alteration of mitochondrial  
167 polarization. The measurement of fluorescence was reported in relative (non-absolute)  
168 fluorescent units (RFU).

169 Rh123 and TMRM fluorescence intensities recorded at the two states of respiration (with or  
170 without substrates) were normalized to the fluorescence recorded after CCCP addition,  
171 according to the following formula:

$$172 \quad 100 - \left( \left( \frac{X - Y}{X} \right) * 100 \right)$$

173 Where: X = Rh123 or TMRM fluorescence intensity after CCCP addition



174 Y = Rh123 or TMRM fluorescence intensity after mitochondria addition with or  
175 without substrates.

176 The calculated normalized fluorescence values using the above formula were based on the  
177 maximum emission value. CCCP at 2  $\mu$ M completely depolarizes mitochondria by consuming  
178 all the proton gradient established by the respiratory chain. As such, the fluorescence intensity  
179 obtained after its addition corresponded only to the dissipation of  $\Delta\Psi_m$ , and made it possible  
180 to take into account the non-specific binding of the dye.

### 181 2.7 Statistical analysis

182 The statistical analysis and graphs were generated with SPSS 17 software. Each experiment  
183 was performed at least in triplicate. Data are expressed as mean  $\pm$  standard deviation.  
184 Unpaired two-sample *t*-tests were used to express the significance of difference ( $p < 0.05$ )  
185 between means, and Levene's test to determine the homogeneity of variance.

## 186 **3. Results**

### 187 *3.1 Changes in the respiratory control index*

188 First, mitochondrial functions in European seabass muscle cells were studied by assessing  
189 mitochondrial respiration. To do this, the respiratory control index (RCI = ADP (state 3) /  
190 CAT) was measured at different *post mortem* storage time points at +4°C (D0 to D8) (**Fig. 1**).  
191 At D0, the RCI value was  $7.3 \pm 1.25$ . At D2, RCI significantly decreased to reach  $4.03 \pm 1.15$ .  
192 From Day 4, the RCI value was near 1: D4 =  $1.34 \pm 0.33$  and D8 =  $1.08 \pm 0.15$ . In short, from  
193 D0 to D4, RCI values gradually decreased to reach the minimum value at D4. From D4, *post*  
194 *mortem* conditions led to mitochondrial respiration disruption.

### 195 *3.2 Changes in membrane potential of isolated mitochondria ( $\Delta\Psi_m$ ) assessed with cationic* 196 *fluorescent probes*

197 The mitochondrial membrane potential of mitochondria isolated from European seabass  
198 muscle cells was assessed at different storage time points: D0 to D7. The two cationic

199 fluorescent probes Rh123 and TMRM were used to evaluate  $\Delta\Psi_m$ . An MVF was required to  
200 record dye fluorescence intensities. The fluorescence intensity of the cationic probes enabled  
201 determination of the  $\Delta\Psi_m$ . When the mitochondrial functions and integrity were preserved,  
202 the generation of  $\Delta\Psi_m$  led to dye stacking inside the mitochondrial matrix. As a consequence,  
203 the fluorescence properties of the cationic probes were affected: fluorescence intensity  
204 decreased (quenching) and emission spectra shifted. In reverse, when mitochondria were  
205 damaged, probe accumulation was weak and fluorescence quenching was low. Therefore, the  
206 level of fluorescence of cationic probes was informative concerning mitochondrial health.

207 Mitochondria isolated from fish muscle at different *post mortem* time points were incubated  
208 with Rh123 in the presence of respiratory substrates (glutamate, malate and succinate)  
209 (**Fig. 2A: black lines**). As a negative control, the protonophore CCCP was added after  
210 mitochondria staining to disrupt  $\Delta\Psi_m$  (**Fig. 2A: red lines**). From D0 to D3, fluorescence  
211 intensities were between 600 and 650 RFU. Then, from D4 to D5, they were higher and  
212 reached 700 RFU. From D6 to D7, fluorescence was recorded at 800 RFU. Thus, from D0 to  
213 D7, fluorescence gradually increased from 600 RFU to 800 RFU, highlighting *post mortem*  
214 disruption of  $\Delta\Psi_m$ . From D0 to D7, the fluorescence intensity recorded after CCCP addition  
215 was always around 900 RFU. This value constituted a reference corresponding to  
216 mitochondria with disrupted  $\Delta\Psi_m$ . From D6 to D7, the values recorded without CCCP (black  
217 curve) were close to those recorded after CCCP addition (red line), showing the strong  
218 disruption of  $\Delta\Psi_m$ . As a negative control, we also stained isolated mitochondria without  
219 respiratory substrates, to confirm that the fluorescence quenching was specifically due to the  
220 energization of mitochondria (data not shown). A blue line has been drawn at 600 RFU to  
221 visualize the significant increasing change in fluorescence intensity from D0-D3 to D4-D7.  
222 These data show  $\Delta\Psi_m$  disruption in the European seabass fish muscle mitochondria after 96  
223 hours of storage at +4°C

224 In order to confirm our results with the Rh123 probe, we used a second cationic fluorescent  
225 probe sensitive to  $\Delta\Psi_m$ . Mitochondria isolated from European seabass muscle cells were  
226 stained with TMRM, following the same protocol used with the Rh123 probe. A typical  
227 fluorescence profile of TMRM after isolated mitochondria labelling was found at different  
228 *post mortem* time points (**Fig. 2B: black lines**). As a negative control, the protonophore  
229 CCCP was added after mitochondria staining to disrupt  $\Delta\Psi_m$  (**Fig. 2B: red lines**). From D0 to  
230 D3, fluorescence intensities were between 700 and 750 RFU. Then, from D4 to D5,  
231 fluorescence was between 1,000 and 1,100 RFU. From D6 to D7, fluorescence reached 1,200  
232 RFU. As such, from D0 to D7, fluorescence gradually increased from 700 RFU to 1,200 RFU,  
233 highlighting *post mortem* disruption of  $\Delta\Psi_m$ . From D0 to D7, the fluorescence intensities  
234 recorded after CCCP addition were between 1,200 and 1,400 RFU. This range of values  
235 constituted a reference corresponding to mitochondria with disrupted  $\Delta\Psi_m$ . From D6 to D7,  
236 the values recorded without CCCP (black curve) were close to those recorded after CCCP  
237 addition (red line), showing the strong disruption of  $\Delta\Psi_m$ . As a negative control, we also  
238 stained isolated mitochondria without respiratory substrates to confirm that the fluorescence  
239 quenching was specifically due to the energization of mitochondria (data not shown). A blue  
240 line has been drawn at 700 RFU to visualize the significant decreasing change in the  
241 quenching fluorescence from D0-D3 to D4-D7. As for Rh123 staining, the data recorded with  
242 the TMRM probe demonstrated  $\Delta\Psi_m$  disruption after 96 hours of storage at +4°C. Therefore,  
243 the results obtained with the TMRM probe were correlated with those recorded with the  
244 Rh123 probe.

### 245 *3.3 Statistical analysis of changes in the fluorescence of cationic probes Rh123 and TMRM at* 246 *different post mortem time points*

247 The experiments illustrated in Figures 2A and 2B were performed at least three times in order  
248 to acquire a statistical overall view of changes in  $\Delta\Psi_m$  at different durations of fish fillet

249 storage (**Fig. 3**). For both probes, fluorescence intensity recorded for each day was normalized  
250 to CCCP. Importantly, the cationic probes Rh123 and TMRM are sensitive to the  $\Delta\Psi_m$ .  
251 However, they can also interact non-specifically with other organelles such as the  
252 endoplasmic reticulum, lysosomes, and other cell fragments (Cottet-Rousselle, Ronot,  
253 Leverage, & Mayol, 2011). This addition of CCCP allowed us to record a fluorescence  
254 intensity in mitochondria with a disrupted mitochondrial membrane. This approach of  
255 rationalization with CCCP therefore enabled us to take into account the non-specific binding  
256 of the dyes.

257 **Fig. 3A** illustrates changes in Rh123 fluorescence normalized to CCCP at different *post*  
258 *mortem* time points. From D0 to D3, normalized Rh123 fluorescence was between 65 and 75  
259 %. From D4 to D7, fluorescence was around 85 %. Two zones delimited by a dotted line at 75  
260 % of fluorescence were identified. This dotted line highlighted a significant change in  $\Delta\Psi_m$   
261 between the two periods: “D0-D3” and “D4-D7”.

262 Changes in TMRM fluorescence were also normalized with CCCP at the same *post mortem*  
263 time points as for the Rh123 probe (**Fig. 3B**). From D0 to D3, normalized TMRM  
264 fluorescence was between 60 and 70 %. From D4 to D7, fluorescence was between 80 and 95  
265 %. Like for the statistical data obtained with the Rh123 probe, a dotted line traced at 75 %  
266 delimited two zones, and highlighted a significant change in  $\Delta\Psi_m$  between the two periods:  
267 “D0-D3” and “D4-D7”.

### 268 *3.4 Evolution of the Rh123 and TMRM fluorescence emission peak wavelengths at different* 269 *post mortem time points*

270 Cationic probe characteristics such as the emission peak wavelength depend on mitochondrial  
271 functions and integrity ((Emaus, Grunwald, & Lemasters, 1986); (Scaduto Jr & Grotyohann,  
272 1999)). For each condition and both probes, emission peak wavelengths were studied with the  
273 MVF (**Fig. 4**).

274 For a given typical experiment with energized mitochondria stained with Rh123, the  
275 fluorescence emission peaks were recorded for each day of storage (**Fig. 4A**). From D0 to D2,  
276 the emission peak wavelength (EPW) was 528 nm. From D3 to D4, the EPW was 526 nm.  
277 Then, from D5 to D7, the EPW was 524 nm. Consequently, from D0 to D7, the emission peak  
278 shifted from 528 nm to 524 nm. As a control, emission fluorescence was measured after  
279 addition of CCCP (524 nm).

280 The emission peak was also recorded at different days of storage after TMRM staining  
281 (**Fig. 4B**). From D0 to D3, the EPW was 579 nm. From D4 to D5, the EPW was 577 nm.  
282 Then, from D6 to D7, the EPW was 576 nm. Consequently, for a given experiment with  
283 energized mitochondria, the TMRM emission profile changed, with a shift from 579 nm to  
284 576 nm from D0 to D7. As a negative control, when mitochondria were decoupled after  
285 CCCP addition, the EPW was 576 nm.

286 For both probes, the EPWs were measured for each duration of storage and compared by  
287 statistical analysis (**Fig. 4C, 4D**). For Rh123 staining (**Fig. 4C**), when mitochondria were  
288 energized, the EPW was higher than 526 nm (527-529 nm) from D0 to D3, and less than 526  
289 nm after 4 days of storage (D4 to D7). A dotted red line on the graph delimited and  
290 highlighted the significant difference between the two zones. When energized mitochondria  
291 were stained with CCCP, emission fluorescence peaks were measured between 524 and 525  
292 nm. As a control, peak emission fluorescence was also recorded between 524 and 525 nm in  
293 the absence of substrates (data not shown). These data demonstrated the specific action of  
294 energized mitochondria on the characteristic emission peak. As a result, the phenomena of  
295 red-shift was only visible with energized mitochondria with respiratory substrates. The same  
296 observations were made for TMRM staining (**Fig. 4D**), except that the wavelength  
297 significantly discriminating D0-D3 from D4-D7 was located at approximately 577.5 nm (**red**  
298 **dotted line: Fig. 4D**).

## 299 **4. Discussion**

300 The development of methods to evaluate fish freshness and thereby its quality is currently still  
301 a challenge and an issue in the fishing industry. In a previous study (Jérôme Cléach, et al.,  
302 2019), we demonstrated that mitochondrial functions and integrity constitute reliable and  
303 early indicators to evaluate gilthead seabream freshness. In the present study, we focused our  
304 experiments on the evaluation of mitochondrial membrane potential ( $\Delta\Psi_m$ ). To this end, we  
305 followed a new approach using an MVF to evaluate  $\Delta\Psi_m$  with cationic fluorescent probes. In  
306 order to study the universality of this method, we performed our experiments on another  
307 farmed species: the European seabass (*Dicentrarchus labrax*). Our results provided  
308 knowledge on *post mortem* mitochondrial bioenergetics in skeletal muscle cells.

### 309 *4.1 Post mortem respiration of mitochondria isolated from fish fillets*

310 As a first approach, we studied mitochondrial functions of European seabass fillet muscle  
311 cells using oxygraphy. The RCI value was calculated to evaluate mitochondrial bioenergetics.  
312 Under given conditions, high RCI indicated good mitochondrial functions, and on the  
313 contrary low RCI usually reflected mitochondrial dysfunction (Brand & Nicholls, 2011). RCI  
314 was therefore a good indicator of mitochondrial health. RCI values were calculated at  
315 different *post mortem* durations of storage: D0, D2, D3, D4 and D8. From D0 to D4, RCI  
316 values gradually decreased. From D4 to D8, the minimum value of RCI was reached,  
317 demonstrating mitochondrial decoupling. In our previous study (Jérôme Cléach, et al., 2019),  
318 the RCI was evaluated using mitochondria isolated from farmed gilthead seabream (*Sparus*  
319 *aurata*) at different durations of storage at +4°C. Comparing the results obtained for both  
320 species, we observed that RCI values were higher in the European seabass model than in the  
321 gilthead seabream model during the initial *post mortem* days. This can be explained by the  
322 fact that RCI values depend on and vary as a function of species and tissues (Hulbert, Turner,  
323 Hinde, Else, & Guderley, 2006). However, for both species, day 4 constituted the critical

324 storage day where mitochondrial functions were significantly disrupted (respiration and  
325  $\Delta\Psi_m$ ).

326 On the one hand, RCI measurement allowed us to validate the high quality of our  
327 mitochondrial extraction protocol. On the other, it made it possible to establish a correlation  
328 between mitochondrial oxygen consumption and  $\Delta\Psi_m$  at different *post mortem* time points.

#### 329 4.2 Post mortem membrane potential of mitochondria isolated from fish fillets

330 As a second approach,  $\Delta\Psi_m$  was assessed at different days *post mortem* using a fluorimetric  
331 method, like for oxygraphy. From D0 to D3, isolated mitochondria conserved their  $\Delta\Psi_m$  in  
332 the presence of respiratory substrates. After 96 h of storage (D4),  $\Delta\Psi_m$  was significantly  
333 disrupted. As a result, there was correlation between changes in mitochondrial respiration and  
334  $\Delta\Psi_m$  in fish muscle cells in *post mortem* conditions. In our previous study, with the gilthead  
335 seabream model, we also demonstrated disruption of  $\Delta\Psi_m$  at D4. Thus, for both species,  
336 mitochondrial bioenergetics were significantly altered at the same *post mortem* time points.  
337 Therefore, D4 represented a “critical” storage time where mitochondrial respiration and  $\Delta\Psi_m$   
338 were significantly and strongly disrupted in both species. This similarity of results can be  
339 explained by the fact that these two species present numerous common points. Importantly,  
340 they have the same lifestyle. Moreover, the tested fish originated from the same aquaculture  
341 farm and consequently had the same nutrition, the same living environment, and were  
342 slaughtered by the same method. All these parameters could probably have a direct impact on  
343 *post mortem* changes in mitochondrial functions and integrity.

#### 344 4.3 The post mortem mitochondrial survival strategy

345 RCI decreased significantly during the first 3 days, with maintenance of the mitochondrial  
346 membrane potential over the same period. On the basis of these results, from D0 to D3,  
347 mitochondria isolated from European seabass fillet muscle cells retained their membrane  
348 potential and the integrity of the respiratory chain. Over the first 3 days, the RCI decreased,

349 illustrating that ADP could no longer accelerate respiratory chains. These results correlate  
350 with those previously obtained on gilthead sea bream (Jérôme Cléach, et al., 2019). From D4  
351 to D8, the RCI decreased significantly and was accompanied by a reduction in membrane  
352 potential to reach its minimum value.

353 The maintenance of  $\Delta\Psi_m$  in *post mortem* conditions (8.5 hours and 24 hours, respectively)  
354 was previously reported by Barksdale, et al. (2010) in other species. In *post mortem*  
355 conditions, muscle cells are deprived of oxygen and nutrients. Similarly, it was reported that  
356 25% of oxygen was still present in beef *longissimus thoracis et lumborum* a few minutes after  
357 slaughtering. After 48 hours of storage at +4°C, 10% of the oxygen was still present in beef  
358 muscle (England, et al., 2018). As mentioned in this study, even a low amount of oxygen and  
359 a low number of viable mitochondria can participate in *post mortem* metabolism. We can  
360 suppose that a certain percentage of oxygen is also present in fish fillets after slaughtering,  
361 and that this allows for survival of mitochondria. Previous studies have clearly shown the key  
362 role of mitochondria in *post mortem* metabolism ((St-Pierre, Brand, & Boutilier, 2000),  
363 (Nicholas J. Hudson, 2012), (England, et al., 2018)). Therefore, mitochondria are selfish and  
364 prioritize their own survival by consuming ATP reserves in order to maintain their  
365 homeostasis and functionality ((St-Pierre, et al., 2000), (Lehmann, Segal, Muradian, &  
366 Fraifeld, 2008), (Nicholas J. Hudson, 2012)). This process of mitochondrial survival in anoxia  
367 is called “mitochondrial treason” (N. J. Hudson, et al., 2017).

#### 368 *4.4 Spectral properties of Rh123 and TMRM as indicators of fish freshness*

369 The originality of this study was based on a new approach to assess mitochondria with an  
370 MVF. This device made it possible to acquire fluorescence emission spectra. We observed  
371 that Rh123 and TMRM fluorescence emissions were strongly impacted as a function of *post*  
372 *mortem* time points. Two characteristics of Rh123 and TMRM are to be considered to  
373 evaluate fish freshness: the level of quenching fluorescence and the emission peak



374 wavelength. From D0 to D3, for both probes, the levels of quenching were higher at the D0-  
375 D3 interval than at the D4-D7 interval. Moreover, the emission fluorescence peak shifts were  
376 only observable at D0-D3, also for both probes. Therefore, mitochondrial probe fluorescence  
377 and emission peaks were linked to the “energized state” of mitochondria. Emaus, et al.,  
378 (1986) were the first to highlight the fluorescence properties of Rh123 using uncoupled and  
379 coupled rat isolated mitochondria. They considered spectral red shifts and fluorescence  
380 quenching to be a consequence of electrophoretic dye uptake, followed by high capacity  
381 binding in the mitochondrial matrix in coupled mitochondria, but not in uncoupled  
382 mitochondria. The same observation was also reported in another study with TMRM  
383 ((Scaduto Jr & Grotyohann, 1999)). These authors showed that TMRM excitation and  
384 emission spectra change, as shown by quenching and peak emission shift, after incubations of  
385 heart rat mitochondria with dye once energized with glutamate, malate and succinate. As  
386 proposed by Diop, et al. (2016), we can also classify in this study a fish fillet in the D0-D3  
387 zone or in the D4-D7 zone, on the basis of high quenching and shift of the fluorescence peak  
388 or high quenching and no shift of the fluorescence peak, respectively. In this way, we  
389 highlighted new markers to evaluate fish freshness. In the future, it may be useful to  
390 investigate whether the fluorescence quenching and the emission peak wavelength shifts  
391 occur in the case of labeling of cells or tissues, as for isolated mitochondria.

## 392 **5. Conclusions**

393 In this study, the respiratory activity and  $\Delta\Psi_m$  of mitochondria isolated from European  
394 seabass fillet were assessed at different *post mortem* time points. Mitochondria were stained  
395 with the cationic probes Rh123 and TMRM, and fluorescence was recorded with an MVF.  
396 We found dysfunction of mitochondrial bioenergetics after 96 hours of storage at +4°C (D4).  
397 Moreover, the spectral properties of the probes, such as emission peak wavelength and  
398 fluorescence intensity, were significantly affected from D4. This study therefore confirmed

399 that evaluation of mitochondrial bioenergetics represents a reliable and early indicator of fish  
400 freshness among the various existing indicators. It would be interesting in the future to  
401 establish a “specific freshness profile” for different fish species, in particular for fish with  
402 high commercial value such as Atlantic salmon (*Salmo salar*) or rainbow trout  
403 (*Oncorhynchus mykiss*).

#### 404 **Funding**

405 This study was funded by the French government, Ifremer and the Hauts-de-France region in  
406 the framework of the CPER 2014-2020 MARCO project.

#### 407 **References**

- 408 Barksdale, K. A., Perez-Costas, E., Gandy, J. C., Melendez-Ferro, M., Roberts, R. C., &  
409 Bijur, G. N. (2010). Mitochondrial viability in mouse and human postmortem brain.  
410 *FASEB J.*, 24(9), 3590-3599.
- 411 Bradford, M. (1976). A rapid and sensitive method for the quantitation of microgram  
412 quantities of protein utilising the principle of protein-dye binding. *Anal. Biochem.*, 72, 248-  
413 254.
- 414 Brand, M. D., & Nicholls, D. G. (2011). Assessing mitochondrial dysfunction in cells.  
415 *Biochem. J.*, 435(2), 297-312.
- 416 Cheng, J. H., Sun, D. W., Han, Z., & Zeng, X. A. (2014). Texture and structure measurements  
417 and analyses for evaluation of fish and fillet freshness quality: a review. *Compr. Rev. Food*  
418 *Sci. Food Saf.*, 13(1), 52-61.
- 419 Cléach, J., Pasdois, P., Marchetti, P., Watier, D., Duflos, G., Goffier, E., Lacoste, A.-S.,  
420 Slomianny, C., Grard, T., & Lencel, P. (2019). Mitochondrial activity as an indicator of  
421 fish freshness. *Food Chemistry*, 287, 38-45.
- 422 Cléach, J., Watier, D., Le Fur, B., Brauge, T., Duflos, G., Grard, T., & Lencel, P. (2018). Use  
423 of ratiometric probes with a spectrofluorometer for bacterial viability measurement. *J.*  
424 *Microbiol. Biotechnol.*, 28(11), 1782-1790.
- 425 Cottet-Rousselle, C., Ronot, X., Leverve, X., & Mayol, J.-F. (2011). Cytometric assessment  
426 of mitochondria using fluorescent probes. *Cytometry Part A*, 79A(6), 405-425.
- 427 Diop, M., Watier, D., Masson, P.-Y., Diouf, A., Amara, R., Grard, T., & Lencel, P. (2016).  
428 Assessment of freshness and freeze-thawing of sea bream fillets (*Sparus aurata*) by a  
429 cytosolic enzyme: Lactate dehydrogenase. *Food Chem.*, 210, 428-434.
- 430 Emaus, R. K., Grunwald, R., & Lemasters, J. J. (1986). Rhodamine 123 as a probe of  
431 transmembrane potential in isolated rat-liver mitochondria: spectral and metabolic  
432 properties. *Biochim. Biophys. Acta, Bioenerg.*, 850(3), 436-448.
- 433 England, E. M., Matarneh, S. K., Mitacek, R. M., Abraham, A., Ramanathan, R., Wicks, J. C.,  
434 Shi, H., Scheffler, T. L., Oliver, E. M., Helm, E. T., & Gerrard, D. E. (2018). Presence of  
435 oxygen and mitochondria in skeletal muscle early postmortem. *Meat Sci*, 139, 97-106.
- 436 Hassoun, A., & Karoui, R. (2015). Front-face fluorescence spectroscopy coupled with  
437 chemometric tools for monitoring fish freshness stored under different refrigerated  
438 conditions. *Food Control*, 54, 240-249.

439 Hudson, N. J. (2012). Mitochondrial treason: a driver of pH decline rate in post-mortem  
440 muscle? *Animal Production Science*, 52(12), 1107.

441 Hudson, N. J., Bottje, W. G., Hawken, R. J., Kong, B., Okimoto, R., & Reverter, A. (2017).  
442 Mitochondrial metabolism: a driver of energy utilisation and product quality? *Animal*  
443 *Production Science*, 57(11), 2204.

444 Hulbert, A. J., Turner, N., Hinde, J., Else, P., & Guderley, H. (2006). How might you  
445 compare mitochondria from different tissues and different species? *Journal of*  
446 *Comparative Physiology B*, 176(2), 93-105.

447 Kuznetsov, A. V., Veksler, V., Gellerich, F. N., Saks, V., Margreiter, R., & Kunz, W. S.  
448 (2008). Analysis of mitochondrial function *in situ* in permeabilized muscle fibers, tissues  
449 and cells. *Nat. Protoc.*, 3(6), 965-976.

450 Lehmann, G., Segal, E., Muradian, K. K., & Fraifeld, V. E. (2008). Do mitochondrial DNA  
451 and metabolic rate complement each other in determination of the mammalian maximum  
452 longevity? *Rejuvenation Res*, 11(2), 409-417.

453 Mendes, R. (2018). Technological processing of fresh gilthead seabream (*Sparus aurata*): A  
454 review of quality changes. *Food Rev. Int.*, 1-34.

455 Mitchell, P. (2011). Chemiosmotic coupling in oxidative and photosynthetic phosphorylation.  
456 1966. *Biochim Biophys Acta*, 1807(12), 1507-1538.

457 Olafsdottir, G., Martinsdóttir, E., Oehlenschläger, J., Dalgaard, P., Jensen, B., Undeland, I.,  
458 Mackie, I., Henahan, G., Nielsen, J., & Nilsen, H. (1997). Methods to evaluate fish  
459 freshness in research and industry. *Trends Food Sci. Technol.*, 8(8), 258-265.

460 Pasdois, P., Parker, J. E., Griffiths, E. J., & Halestrap, A. P. (2011). The role of oxidized  
461 cytochrome c in regulating mitochondrial reactive oxygen species production and its  
462 perturbation in ischaemia. *Biochemical Journal*, 436(2), 493-505.

463 Perry, S. W., Norman, J. P., Barbieri, J., Brown, E. B., & Gelbard, H. A. (2011).  
464 Mitochondrial membrane potential probes and the proton gradient: a practical usage guide.  
465 *Biotechniques*, 50(2), 98-115.

466 Rehbein, H., & Oehlenschläger, J. (2009). *Fishery products: quality, safety and authenticity*:  
467 John Wiley & Sons.

468 Scaduto Jr, R. C., & Grotyohann, L. W. (1999). Measurement of mitochondrial membrane  
469 potential using fluorescent rhodamine derivatives. *Biophysical journal*, 76(1), 469-477.

470 St-Pierre, J., Brand, M. D., & Boutilier, R. G. (2000). Mitochondria as ATP consumers:  
471 cellular treason in anoxia. *Proc. Natl. Acad. Sci. U. S. A.*, 97(15), 8670-8674.

472 Wu, L., Pu, H., & Sun, D.-W. (2019). Novel techniques for evaluating freshness quality  
473 attributes of fish: A review of recent developments. *Trends in Food Science & Technology*,  
474 83, 259-273.

475 Zorova, L. D., Popkov, V. A., Plotnikov, E. Y., Silachev, D. N., Pevzner, I. B., Jankauskas, S.  
476 S., Babenko, V. A., Zorov, S. D., Balakireva, A. V., & Juhaszova, M. (2018).  
477 Mitochondrial membrane potential. *Analytical biochemistry*, 552, 50-59.

478

479 **Figures caption**

480 **Fig. 1:** Changes in the respiratory control index (RCI) of mitochondria isolated from  
481 European seabass fillet muscle cells at different *post mortem* storage times at +4°C  
482 Letters denote values that are significantly different at different storage times. The *t*-test was  
483 performed using the SPSS Statistics 17 system. The different letters (a, b, c, d) above each bar  
484 represent significant differences; ( $p < 0.05$ ;  $n=3$ ).

485

486 **Fig. 2:** Changes in  $\Delta\Psi_m$  of European seabass fillet muscle cell-isolated mitochondria assessed  
487 with the Rh123 (A) or TMRM (B) probes

488 A: Rh123 probe: relative fluorescence units were measured at different time points of *post*  
489 *mortem* storage at +4°C (from Day 0 to Day 7).  $\Delta\Psi_m$  was evaluated in the presence of  
490 substrates without (dark lines) or with (red lines) CCCP. The blue line highlights the  
491 significant change in membrane potential between the periods D0 to D3 and D4 to D7

492 B: TMRM probe: relative fluorescence units were measured at different time points of *post*  
493 *mortem* storage at +4°C (from Day 0 to Day 7).  $\Delta\Psi_m$  was evaluated in the presence of  
494 substrates without (dark lines) or with (red lines) CCCP. The blue line highlights the  
495 significant change in membrane potential between the periods D0 to D3 and D4 to D7.

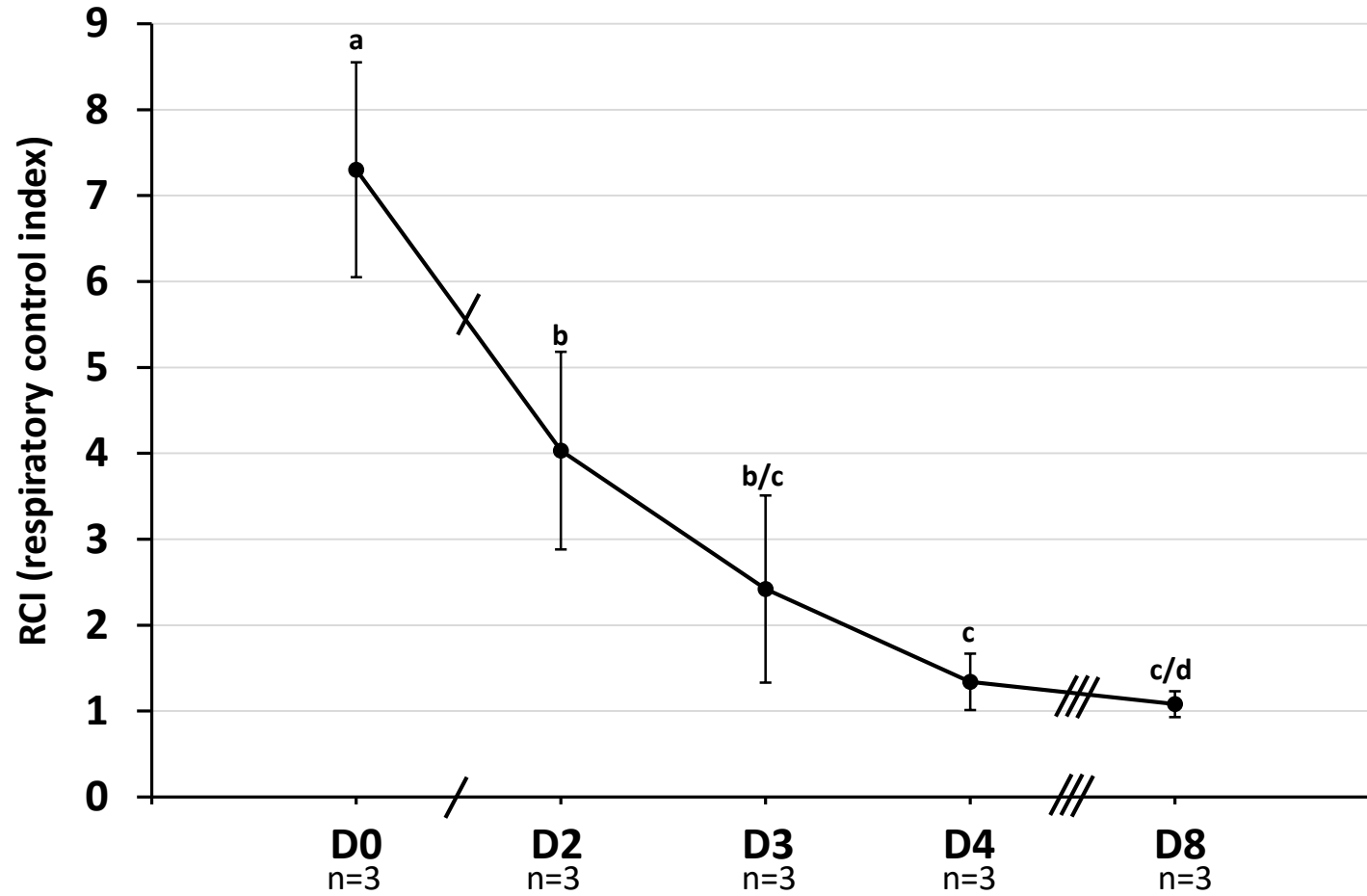
496

497 **Fig. 3:** Summary graphs of Rh123 (A) or TMRM (B) fluorescence levels normalized to CCCP  
498 at different storage times

499 The different letters (a, b, c) represent significant differences; ( $p < 0.05$ ;  $n=3-6$ ). The dotted  
500 line highlights the significant change in membrane potential between the periods D0 to D3  
501 and D4 to D7.

502

503 **Fig. 4:** Changes in the Rh123 (A) and TMRM (B) fluorescence emission peak wavelengths as  
504 a function of different storage times of seabass fillets and their statistical representations (C  
505 and D)  
506 Figures A and B are representative of a typical experiment.  
507 The different letters (a, b, c, d) above each bar (C and D) represent significant differences; ( $p$   
508  $< 0.05$ ;  $n=3$ ).  
509 The blue vertical lines indicate the wavelengths 528 nm (A) or 579 nm (B), corresponding to  
510 the fluorescence peak after staining of mitochondria isolated from fish fillet muscle cells  
511 between D0 and D3.  
512 The grey vertical lines indicate the wavelengths 524 nm (A) or 576 nm (B), corresponding to  
513 the fluorescence peak after staining of mitochondria isolated from fish fillet muscle cells  
514 between D4 and D7.  
515 The red vertical dotted lines (A and B) highlight the limit between two mitochondrial  
516 functional states.  
517 The blue curves (C and D) illustrate changes in the fluorescence emission peak wavelengths  
518 in the presence of stained mitochondria from D0 to D7.  
519 The grey curves (C and D) illustrate changes in the fluorescence emission peak wavelengths  
520 in the presence of stained mitochondria and CCCP from D0 to D7.  
521 The red horizontal dotted lines (C and D) highlight the limit between two mitochondrial  
522 functional states.

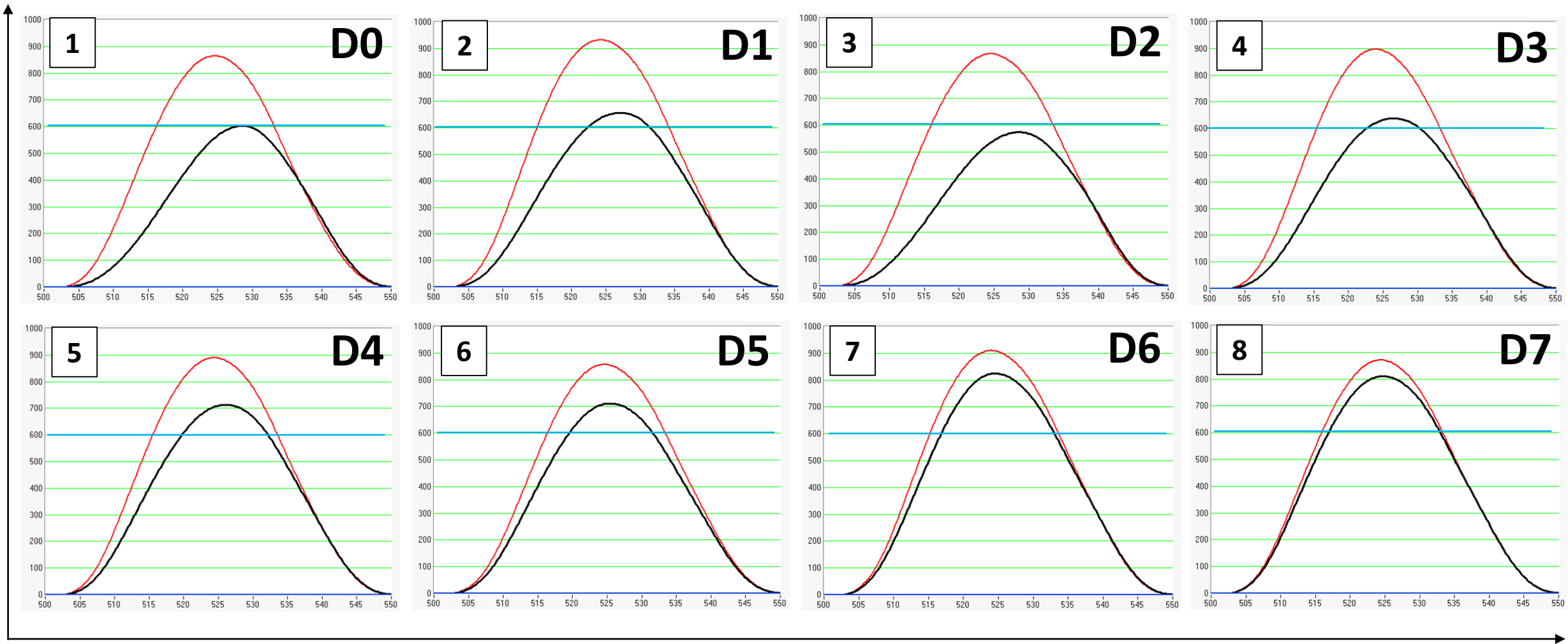


<i>Day of storage</i>					
	<b>D0</b>	<b>D2</b>	<b>D3</b>	<b>D4</b>	<b>D8</b>
<i>RCI value</i>	7.3 ± 1.25	4.03 ± 1.15	2.42 ± 1.09	1.34 ± 0.33	1.08 ± 0.15

# Rh123

**A**

**Relative fluorescence units (RFU)**



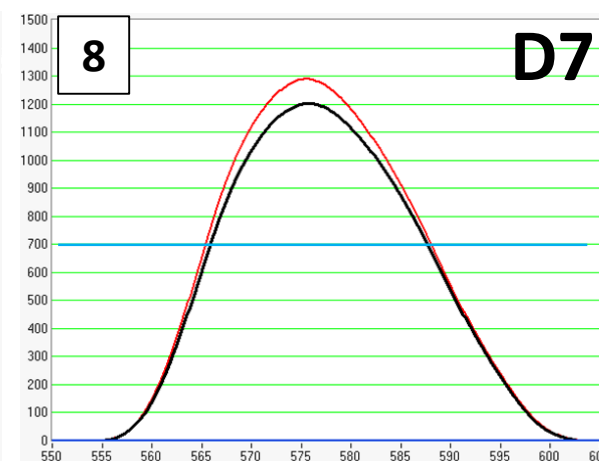
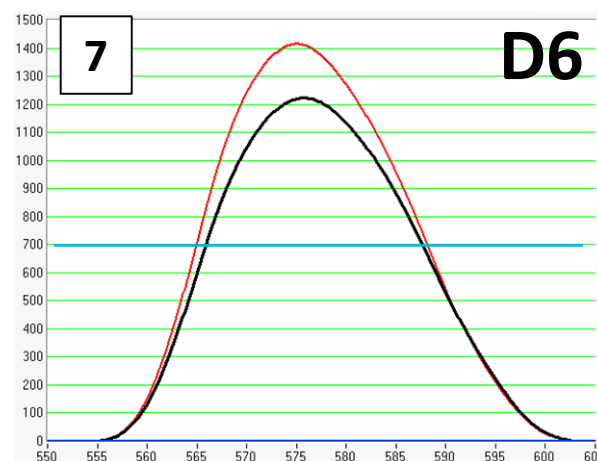
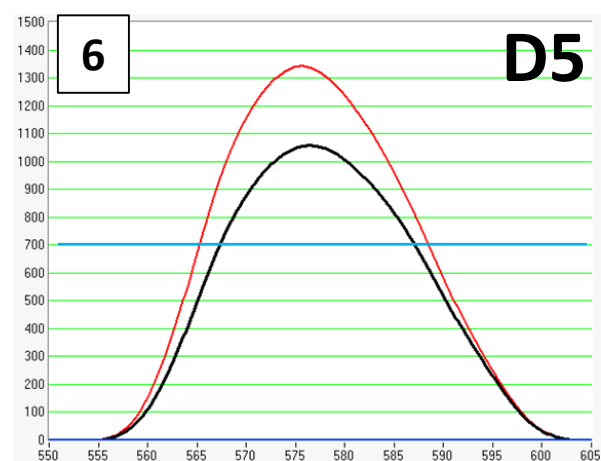
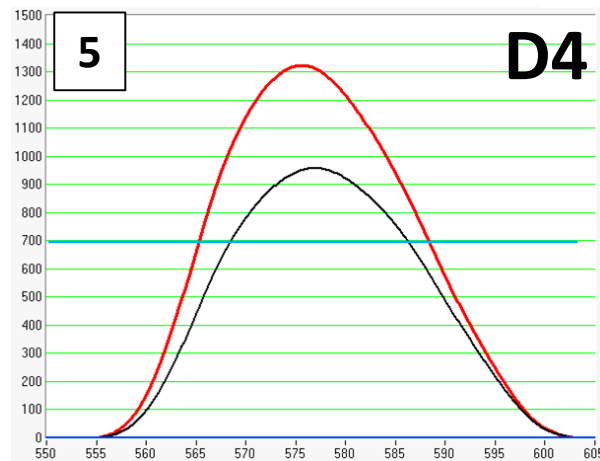
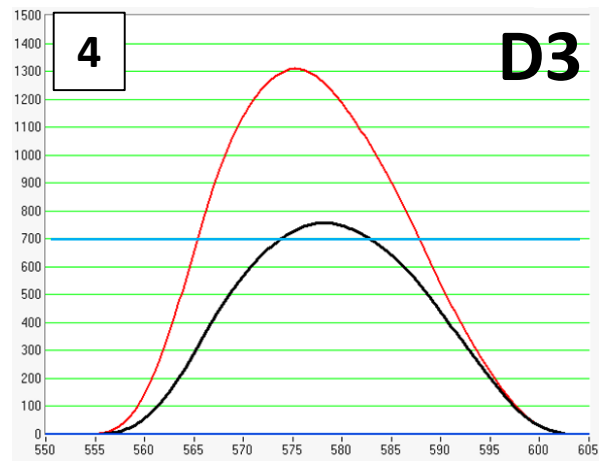
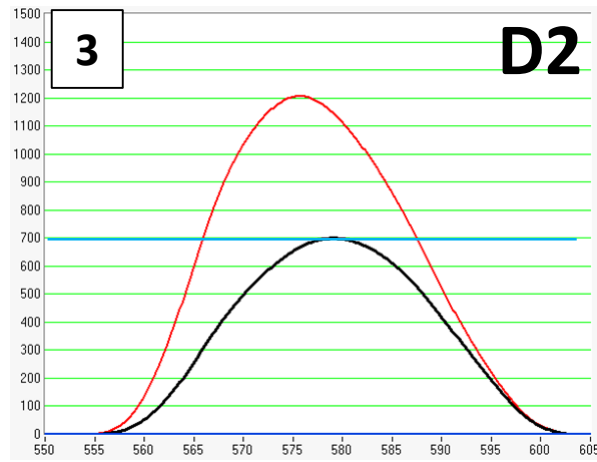
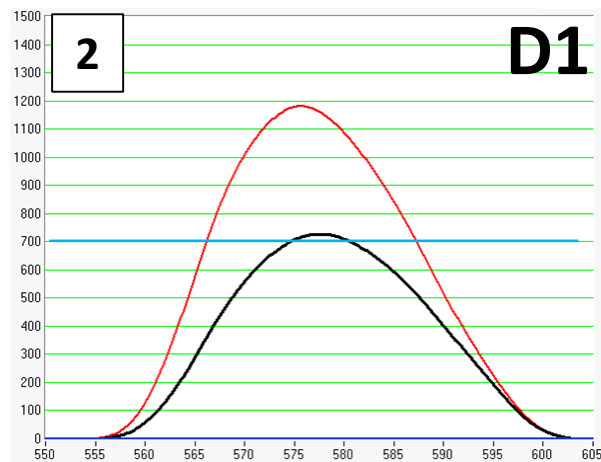
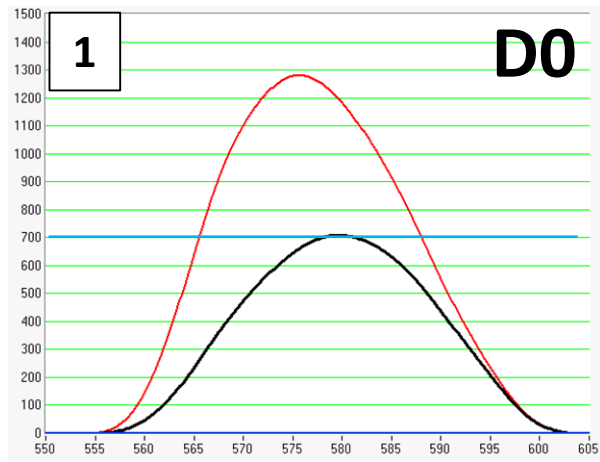
**Wavelengths (nm)**

— Substrates without CCCP    — Substrates with CCCP

# TMRM

**B**

Relative fluorescence units (RFU)



Wavelengths (nm)

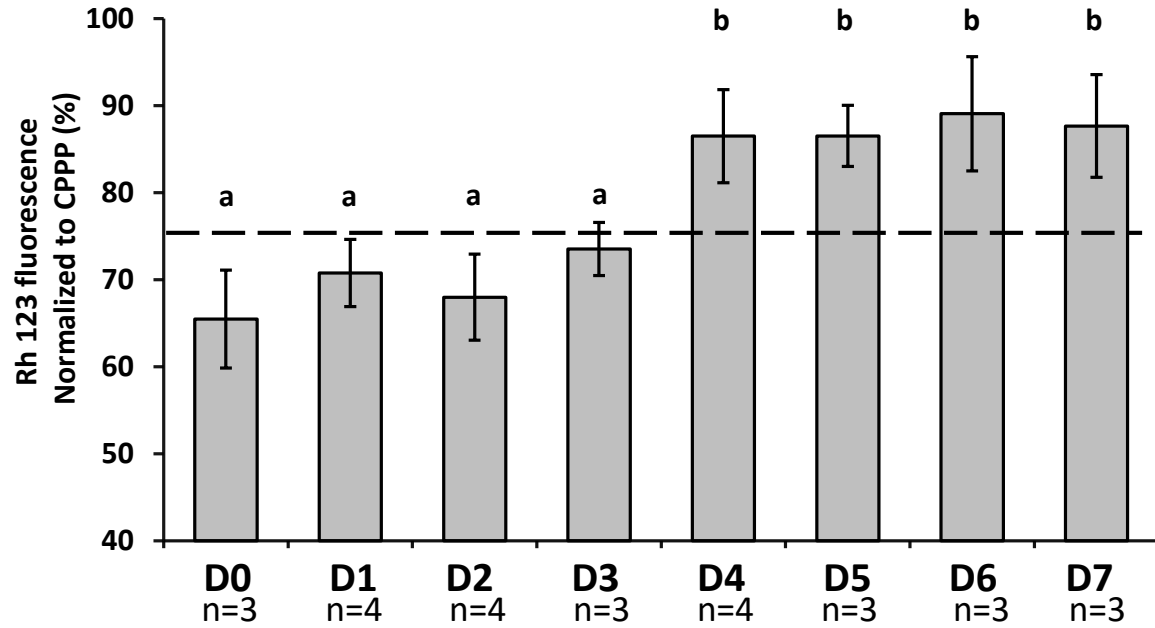
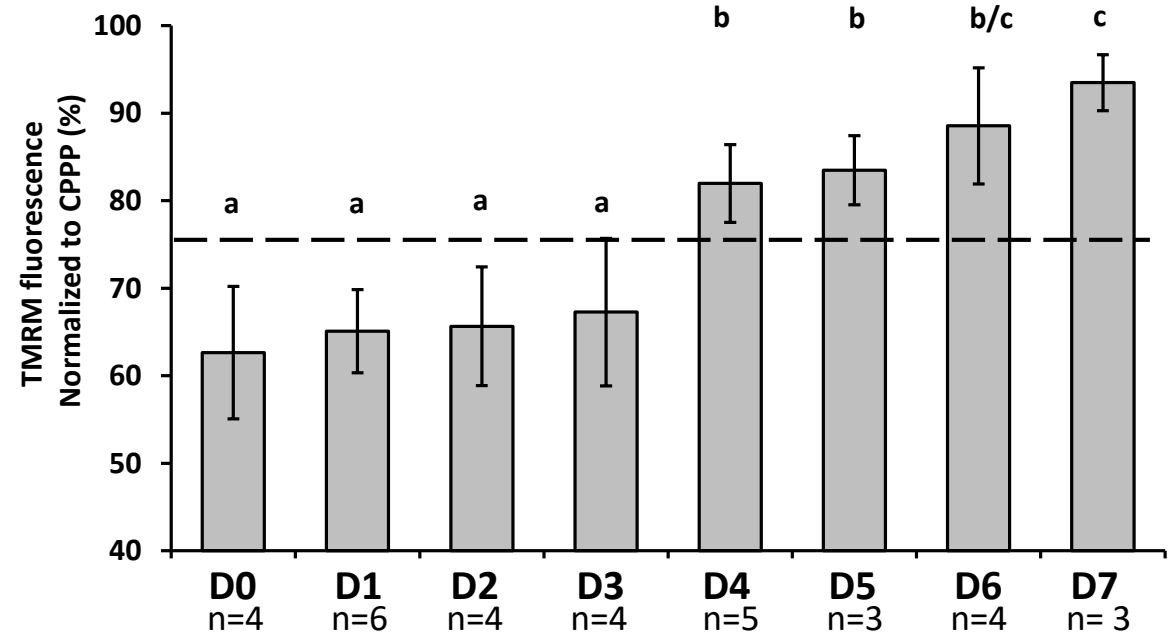


Substrates without CCCP



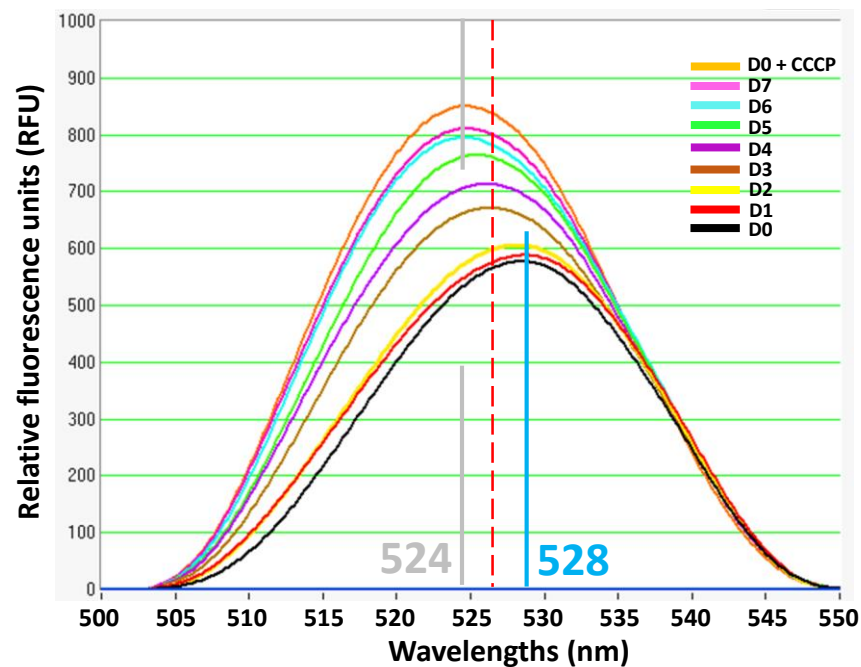
Substrates with CCCP



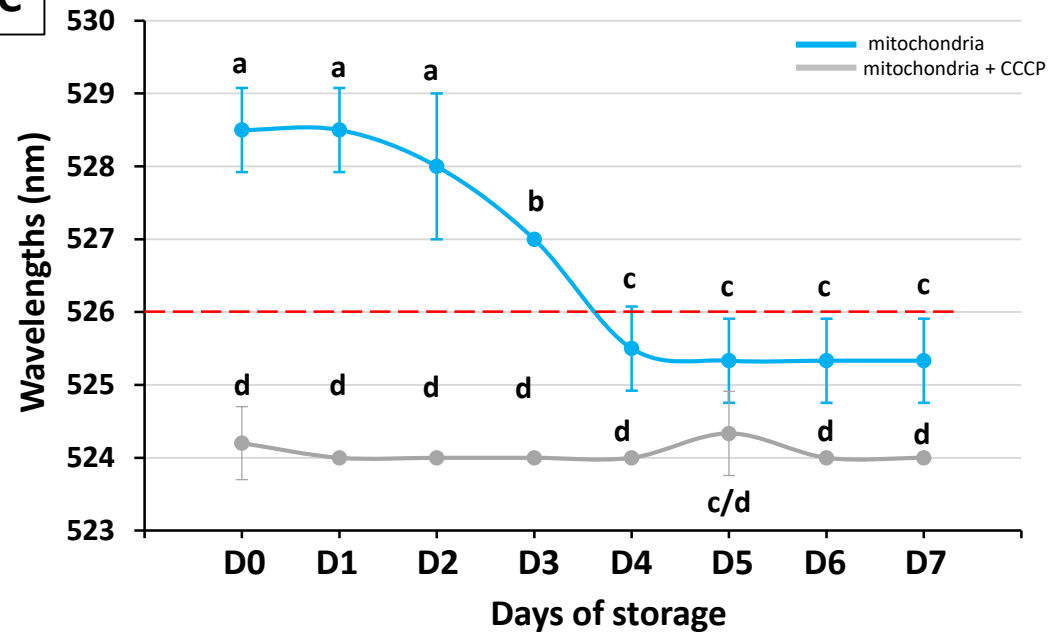
**A****Rh123****B****TMRM**

**Rh123**

**A**

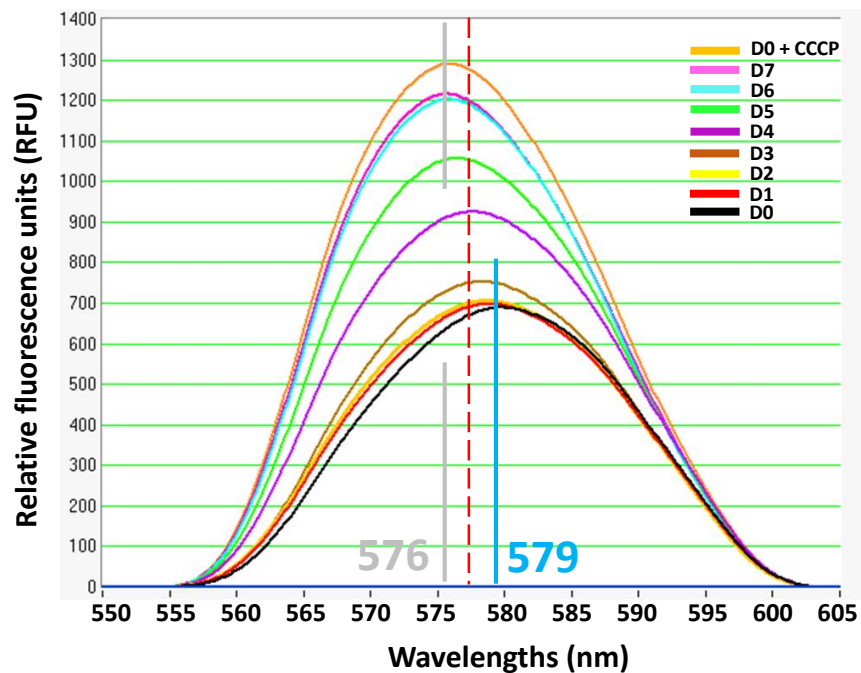


**C**



**TMRM**

**B**



**D**

